Acta Crystallographica Section B
Structural Science
ISSN 0108-7681

Redetermination, invariom-model and multipole refinement of L-ornithine hydrochloride

B. Dittrich,* P. Munshi and M. A. Spackman

Department of Chemistry, M313, School of Biomedical, Biomolecular and Chemical Sciences, University of Western Australia, Crawley, WA 6009, Australia

Correspondence e-mail: birger@cyllene.uwa.edu.au

Received 31 January 2007
Accepted 27 March 2007

The structure of L-ornithine hydrochloride, $C_5H_{13}N_2O_2^+Cl^-$, has been redetermined at 100 K by single-crystal X-ray diffraction within a project that aims to generate accurate bond-distance restraints for the invariom refinement of proteins. The high-resolution data were subject to an invariom and a multipole refinement, and the resulting electron densities on a grid were compared. Improvements in the conventional *R* factor obtained by multipole modelling were smaller than in other structures containing solely the elements CHNO owing to Cl core scattering. Cruickshank's diffraction-component precision index and Stevens & Coppens suitability factor are discussed.

1. Introduction

L-Ornithine is a non-standard amino acid that induces the release of growth hormones, encourages muscle building and plays an important role in mammalian metabolism in the Krebs cycle. L-Ornithine occurs in many protein, oligopeptide and antibiotic molecules, although it is not encoded by the human genome. The X-ray crystal structure of L-ornithine hydrochloride was first determined by Chiba *et al.* (1967). In this study we make use of redetermined diffraction data of excellent quality and compare the structure and figures-of-merit from invariom modelling (Dittrich *et al.*, 2004), which invokes the Hansen & Coppens multipole model (Hansen & Coppens, 1978), with those from the independent atom model (IAM). In marked contrast to the significant improvements obtained in earlier studies using data of similar quality (Kingsford-Adaboh *et al.*, 2006; Dittrich, Munshi & Spackman, 2006), the improvement in the *R* factor in this study was modest. The differences between this work and earlier studies have been investigated. The assigned invariom electron density was directly compared with the refined multipole model electron density on a grid. *R*-factor improvements gained by multipole modelling are discussed in light of Stevens & Coppens' (1976) suitability factor and Cruickshank's diffraction-component precision index (DPI) value.

The modelling of experimental diffraction data with transferable, experimentally derived, non-spherical scattering factors was first performed in the early nineties (Brock *et al.*, 1991). Koritsánszky *et al.* (2002) have shown that non-spherical scattering factors can be obtained by following a purely theoretical methodology. The application of the experimental (Jelsch *et al.*, 1998; Zarychta *et al.*, 2007) or theoretical databases (Dittrich, Hübschle, Luber & Spackman, 2006; Volkov *et al.*, 2007) to oligopeptide data promises interesting future applications in protein crystallography.

2. Experimental

The X-ray crystal structure of L-ornithine hydrochloride, together with L-ornithine hydrobromide, was first determined by Patterson methods (Chiba *et al.*, 1967); our atomic numbering scheme (Fig. 1*a*) and unit-cell settings follow the original publication. The results of a Cambridge Structural Database (Allen, 2002) search for structures

Table 1
Experimental details.

Crystal data			
Chemical formula	$C_5H_{13}N_2O_2{\cdot}Cl$		
M_r	168.62		
Cell setting, space group	Monoclinic, $P2_1$		
Temperature (K)	100		
a, b, c (Å)	9.9480 (2), 7.9637 (2), 4.9826 (1)		
β (°)	83.13 (1)		
V (Å^3)	391.91 (2)		
Z	2		
D_x (Mg m^{-3})	1.429		
Radiation type	Mo $K\alpha$		
μ (mm^{-1})	0.43		
Crystal form, colour	Rectangle, colourless		
Crystal size (mm)	0.71 × 0.63 × 0.24		
Data collection			
Diffractometer	Oxford Diffraction Xcalibur S		
Data collection method	ω scans		
Absorption correction	Analytical		
T_{min}	0.790		
T_{max}	0.914		
$(\sin\theta/\lambda)_{max}$ (Å^{-1})	1.12		
No. of measured, independent and observed reflections	34 435, 8892, 8123		
Criterion for observed reflections	$F > 3\sigma(F)$		
N_{ref}/N_{var}	15.2		
R_{int}	0.020		
θ_{max} (°)	52.7		
Intensity decay (%)	Not observed		
	Multipole	Invariom	IAM
Refinement			
Refinement on	F	F	F
$R_1(F)$	0.0131	0.0136	0.0180
$wR(F)$	0.0083	0.0089	0.0159
$R_{all}(F)$	0.0184	0.0195	0.0201
S	1.68	1.80	3.21
$\Delta\rho_{max}$, $\Delta\rho_{min}$ (e Å^{-3})	0.30, −0.43	0.33, −0.45	0.55, −0.35
No. of parameters	238	143	143
No. of reflections	8123		
H-atom treatment	Refined independently		
Weighting scheme	$w = 1/[\sigma^2(F_o)]$		
$(\Delta/\sigma)_{max}$	< 0.0001		
Absolute structure	Dittrich, Strümpel, Koritsánszky, Schäfer & Spackman (2006) and Flack (1983)		
Flack parameter	–	−0.00 (7)	0.01 (12)

Computer programs used: *CrysAlis CCD* (Oxford Diffraction, 2006), *XD* Koritsánszky *et al.* (2003), *PLATON* (Spek, 2003), *publCIF* (Westrip, 2007).

containing the ornithine fragment are included in the supplementary information. Single crystals of L-ornithine hydrochloride (purchased from Sigma Aldrich) were grown by vapour diffusion of acetone into an aqueous saturated solution of the title compound. Data collection was carried out on an Oxford Diffraction Xcalibur S diffractometer with Mo $K\alpha$ radiation, each frame covering 1° in ω. *CrysAlis Red* (Oxford Diffraction, 2006) was used for data reduction and for the face-indexed analytical absorption correction (Clark & Reid, 1995). Crystallographic data can be found in Table 1.

3. Pseudoatom modelling

The refinement of L-ornithine hydrochloride was initiated with the original structure (Chiba *et al.*, 1967), omitting H atoms and using isotropic displacement parameters. The 13 H atoms were found as the 13 highest peaks in the difference Fourier map. An IAM refinement with *SHELXL*97 (Sheldrick, 1997) provided starting values for subsequent refinements. Non-spherical atom and IAM refinements, which included reflections with $F>3\sigma(F)$, were both performed with *XDLSM* as included in the *XD* package (Koritsánszky *et al.*, 2003). *XD* input files were processed with the program *InvariomTool* (Hübschle *et al.*, 2007). In all refinements the chloride ion was modelled as spherical and was assigned a charge of −1. For invariom refinement non-spherical valence scattering contributions for C, N and O atoms were obtained from theoretical calculations on model compounds that included nearest-neighbour atoms, whereas H-atom model compounds also included the next-nearest neighbour atoms. The basis set D95++(3df,3pd) was used to optimize the geometry of these model compounds with the program *GAUSSIAN*98 (Frisch *et al.*, 2002). The deviation from electroneutrality was 0.40 electrons out of 62 valence electrons and electroneutrality was achieved by scaling H atom monopoles only. Full details for the general invariom modelling procedure of organic molecules can be found in Hübschle *et al.* (2007).

The choice of local atomic site symmetry and the values of the multipole parameters of the invariom database served as starting values for a multipole refinement, *i.e.* the same local atomic site symmetry was used for both refinements. This led to 96 additional multipole parameters in the multipole refinement; kappa parameters were fixed to invariom database values to allow a direct comparison of the density as shown in Fig. 1(*b*) and discussed below. Since in the invariom refinement the multipole parameters are fixed at theoretically predicted values, only the 142 positional and displacement parameters, as well as the Flack parameter, were refined. In the multipole refinement l_{max} for H atoms was limited to 1, and the 39 hydrogen positional parameters as well as their higher multipoles were not refined but kept at invariom results. Details of the multipole model in terms of local atomic site symmetry and chemical equivalence ('chemical constraints') and of the model compounds used for predicting the aspherical electron density for invariom refinement are specified in Table 2. A Flack parameter was only determined in the invariom and IAM refinements. The supplementary information contains deformation electron density maps from experimental and invariom refinement as well as residual density maps, the latter also from IAM refinement.

4. Results and discussion

Invariom modelling aims to replace the IAM for crystal structures of organic compounds by theoretically predicted non-spherical pseudoatom scattering factors that are transferable from one molecule to another. S, P and Cl, Br occur frequently in organic structures and all have a dominant core scattering contribution. The dominance of the

[1] Supplementary data for this paper are available from the IUCr electronic archives (Reference: SN5050). Services for accessing these data are described at the back of the journal.

Table 2
Details of invariom and multipole refinement.

Atom	Invariom assigned	Site symmetry	Model compound	Chemical constraints
Cl1	Cl^-	6	Chloride ion	–
O1	O1.5c[1.5o1c]$^-$	*m*	Formic acid anion	
O2	O1.5c[1.5o1c]$^-$	*m*	Formic acid anion	O1
N1	N1c1h1h1h$^+$	3	Methylamide cation	
N2	N1c1h1h1h$^+$	3	Methylamide cation	N1
C1	C1.5o1.5o1c$^-$	*m*	Formic acid anion	
C2	C1n1c1c1h	*m*	Aminopropane	
C3	C1c1c1h1h	*mm*2	Propane	
C4	C1c1c1h1h	*mm*2	Propane	C3
C5	C1n1c1h1h	1	Aminoethane	
H1	H1n[1c1h1h]$^+$	6	Methylamide cation	
H2,3,11–13	H1n[1c1h1h]$^+$	6	Methylamide cation	H1
H4	H1c[1n1c1c]	6	Aminopropane	
H5	H1c[1c1c1h]	6	Propane	
H6–8	H1c[1c1c1h]	6	Propane	H5
H9	H1c[1n1c1h]	6	Aminoethane	
H10	H1c[1n1c1h]	6	Aminoethane	H9

Table 3
Bond distances for multipole-, invariom- and IAM refinements and differences between them multiplied by 10^2 with Δ_1 = distance(invariom) − distance(IAM), Δ_2 = distance(multipole) − distance(IAM) and Δ_3 = distance(multipole) − distance(invariom).

Bond lengths involving H atoms for the multipole refinement were kept at the invariom results.

Bond	Multipole	Invariom	IAM	Δ_1	Δ_2	Δ_3
O1—C1	1.2599 (3)	1.2601 (2)	1.2614 (4)	−0.13	−0.15	0.02
O2—C1	1.2503 (3)	1.2495 (2)	1.2513 (4)	−0.18	−0.10	0.08
N1—C2	1.4882 (3)	1.4890 (2)	1.4901 (4)	−0.11	−0.19	−0.08
N2—C5	1.4903 (3)	1.4906 (3)	1.4908 (4)	−0.02	−0.05	−0.03
C1—C2	1.5397 (3)	1.5383 (2)	1.5391 (4)	−0.08	0.06	0.14
C2—C3	1.5322 (3)	1.5321 (3)	1.5310 (5)	0.11	0.12	0.01
C3—C4	1.5214 (3)	1.5212 (3)	1.5217 (5)	−0.05	−0.03	0.02
C4—C5	1.5193 (3)	1.5187 (3)	1.5187 (5)	0.0	0.06	0.06
N1—H1	–	1.020 (6)	0.836 (9)	18.4	–	–
N1—H2	–	1.008 (5)	0.857 (7)	15.1	–	–
N1—H3	–	1.036 (5)	0.864 (8)	17.2	–	–
N2—H11	–	1.034 (6)	0.869 (8)	16.5	–	–
N2—H12	–	1.019 (6)	0.886 (8)	13.3	–	–
N2—H13	–	1.017 (5)	0.879 (8)	13.8	–	–
C2—H4	–	1.068 (4)	0.932 (7)	13.6	–	–
C3—H5	–	1.079 (5)	0.991 (7)	8.8	–	–
C3—H6	–	1.089 (5)	0.950 (7)	13.9	–	–
C4—H7	–	1.085 (5)	0.981 (7)	10.4	–	–
C4—H8	–	1.087 (4)	0.984 (7)	10.3	–	–
C5—H9	–	1.051 (5)	0.963 (7)	8.8	–	–
C5—H10	–	1.086 (5)	0.921 (7)	16.5	–	–

core scattering of the Cl ion is responsible for the relatively small improvement of the invariom model *R* factor of 1.36 with respect to the already excellent IAM *R* factor of 0.0180 (Table 1) for L-ornithine hydrochloride. This is supported by the fact that the multipole refinement does not improve the *R* factor (0.0131) significantly with respect to the invariom model, although the former incorporates the effects of hydrogen bonding. In addition, the highest peak in the residual density is almost the same (multipole: 0.30, invariom: 0.33 e Å^{-3}) in both refinements.

An *ORTEP* plot of molecular structure and the atomic labelling scheme is depicted in Fig. 1(*a*) using the result of the invariom refinement. Fig. 1(*b*) visualizes the difference between the static electron densities obtained from a multipole refinement and the invariom refinement on a grid calculated with the utility *ADDGRID* of the *XD* package (Koritsánszky *et al.*, 2003). Small differences are seen at the Cα hydrogen H4, at the carboxylate group and close to the Cγ—Nδ bond. Differences around the carboxylate group O atom can be attributed to hydrogen bonding, an indication that the crystal field effect can be studied using this methodology, which we will pursue in subsequent work. Fig. 1(*b*) shows that the multipole-model and the invariom-model electron density are equivalent, as the highest differences are only around 0.1 e Å^{-3}, significantly less than the largest residual electron density of 0.3 e Å^{-3}. It has to be pointed out that this difference density is not a residual electron density based on Fourier methods, as only modelled features of the two refinements are considered.

One of the benefits of the invariom model is that molecular geometries resemble those derived from the experimental multipole refinement. A comparison of bond lengths from IAM, invariom and multipole refinements is given in Table 3, from where it can be observed that the differences between invariom and multipole model are small. In addition, signs and magnitudes of the differences between IAM–invariom and IAM–multipole are, except for the C1—C2 bond, alike. As the bonding density between atoms is taken into

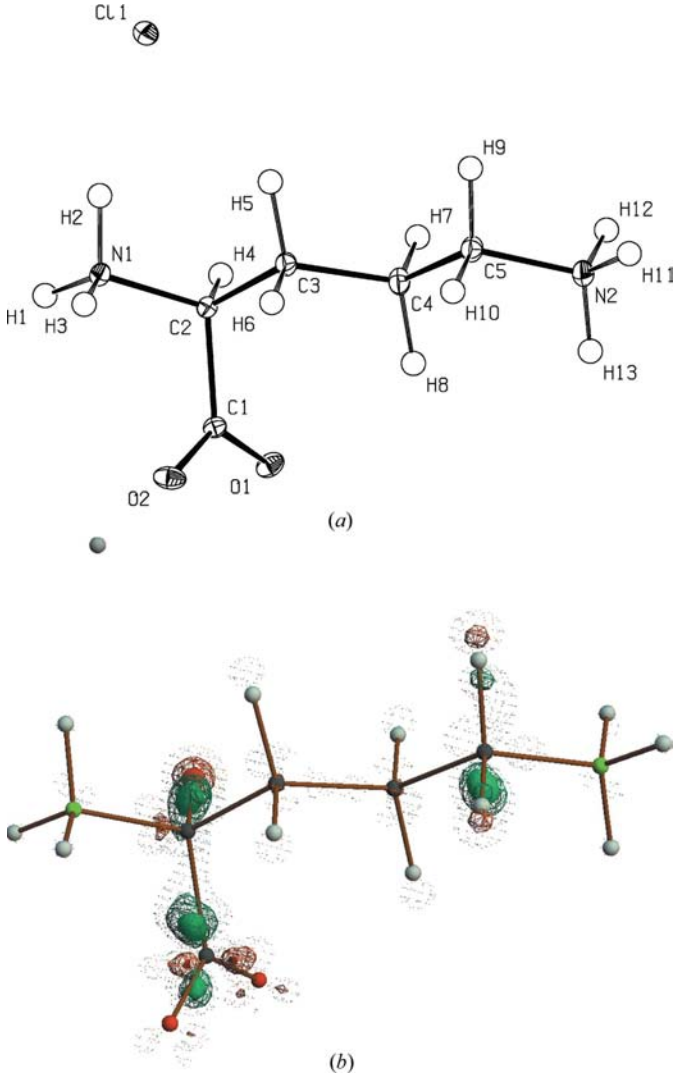

Figure 1
(*a*) *ORTEP* representation (Burnett & Johnson, 1996) of the experimentally determined molecular structure in the crystal with atomic numbering scheme and displacement ellipsoids with 50% probability. (*b*) Calculated difference between multipole and invariom refinement. This difference is not a residual density map, as only modelled features are considered. Isosurfaces are 0.05 (dotted), 0.075 (meshed) and 0.1 (filled). Positive features are shown in green, negative surfaces in red.

Table 4
Suitability factors for five example structures and differences Δ_R between $R(F)$ for IAM and invariom refinements.

Compound	Formula sum	S	Δ_R
L-Ornithine hydrochloride	$C_5H_{13}N_2O_2Cl$	1.44	0.44
4-*O*-Methylalpinumisoflavone	$C_{21}H_{18}O_5$	4.03	1.72
O,*O*-Dimethylalpinumisoflavone	$C_{22}H_{20}O_5$	4.14	1.52
5-*O*-Methyl-4-*O*-(3-methylbut-2-en-1-yl)alpinum-isoflavone	$C_{26}H_{26}O_5$	4.48	1.61
L-Valinol	$C_5H_{13}NO$	5.72	1.34

account locally by multipole modelling rather than by a spherical average in the IAM, the difference invariom–IAM usually shows longer X—H and shorter X—X bonds (X = C, N, O). Improvements are obvious for X—H bond lengths, as discussed earlier (Dittrich *et al.*, 2005). It can furthermore be seen that standard uncertainties in the invariom refinement are reduced (Table 3) with respect to the IAM. Typical changes in *e.g.* C—O bond lengths are less obvious and often not larger than three standard uncertainties.

ADPs from an invariom refinement are less contaminated by bonding electron density than in the IAM. This is supported by the results of the Hirshfeld test (Hirshfeld, 1976). In the IAM the C2—O2 bond fails this test, as the difference of the mean-square displacement amplitude (DMSDA) exceeds 10×10^{-4} Å^2, and the average value is 5.6×10^{-4} Å^2. After invariom modelling, the average is 1.5×10^{-4} Å^2 and no pairs of atoms fail the test, leading to the same result of the multipole refinement. Improvements in geometry and the anisotropic displacement parameters remain even when the dominant scattering contribution of heavier atoms leads to comparably small improvements in the figures-of-merit.

Invariom refinement has previously been shown (Dittrich, Strümpel, Koritsánszky, Schäfer & Spackman, 2006) to reduce the standard deviations of the Flack parameter (Flack, 1983). Owing to the anomalous scattering of the chloride ion, the absolute structure and the chirality of the ornithine molecule can be determined accurately by the IAM. The standard uncertainty and the Flack parameter obtained from the IAM refinement, 0.01 (12), were however improved to 0.00 (7) by invariom refinement.

4.1. What *R*-factor improvements can be expected from invariom refinement?

Stevens & Coppens (1976) have introduced a suitability factor for charge-density studies.

$$S = \frac{V}{\sum_i^{\text{unit cell}} n_{\text{core},i}^2} \qquad (1)$$

The suitability factor relates the suitability S of a compound with the ratio of unit-cell volume V and core scattering as approximated with the sum of the squares of the number of core electrons (n_{core}^2) for atoms of type i. It is based on the observation that improvements resulting from the use of the multipole model are mainly due to the better description of the valence electron density. Hence, the suitability of a structure for multipole refinement decreases as the influence of core scattering increases. For the title structure and four other structures studied by invariom modelling recently (Kingsford-Adaboh *et al.*, 2006; Dittrich, Munshi & Spackman, 2006), the suitability factors were calculated and are listed in Table 4, ordered by their suitability factor.

Whereas the suitability factor indicates where *R*-factor differences Δ_R, $\Delta_R = R_{\text{iam}} - R_{\text{invariom}}$ (Table 4), are likely to be modest because of dominant core scattering, it does not predict how well the spherically averaged IAM valence density resembles the real density. It is therefore not directly proportional to *R*-factor differences Δ_R for data of similar resolution and quality.

Cruickshank's diffraction component precision index (DPI), see (2) (Cruickshank, 1999), can provide an approximate estimation of the standard uncertainties.

$$\text{DPI} = \sigma(x, B_{\text{avg}}) = [N_i/(n_{\text{obs}} - n_{\text{par}})]^{1/2} \cdot C^{-1/3} \cdot R(F) \cdot d_{\min} \qquad (2)$$

In (2) N_i is the number of atoms of type i possessing a scattering power similar to the j atoms in the asymmetric unit as in $\sum_j f_j^2 = N_i f_i^2$, n_{obs} and n_{par} are the number of observations and parameters, C is the percentage of completeness and $d_{\min}$ is the resolution of the experiment. Apart from providing approximate standard uncertainties, the DPI can indicate whether an oligopeptide or protein structure is suitable for invariom refinement (Dittrich, Hübschle, Luger & Spackman, 2006), as it roughly correlates the improvements that can be expected in the figures-of-merit (Δ_R) with data quality and information content of a data set. However, the DPI does not take into account model inadequacies, like the spherical averaging of valence electron density in the IAM that it includes *via* $R(F)$. It would therefore be desirable to combine the suitability factor of (1) with the DPI of (2). As the suitability factor cannot quantify the performance of the IAM, combining both factors in a simple empirical relation that predicts Δ_R remains difficult.

5. Conclusion

In this work we discuss the 'suitability' of a structure for aspherical-atom refinement using the example of L-ornithine hydrochoride. In case heavier atoms occur in a structure, dominating the scattering of a structure by their core electrons, the improvement in the *R* factor by multipole or invariom refinements is smaller than for structures containing only first-row elements. It is therefore useful to adjust expectations with respect to improvements of figures-of-merit by invariom modelling when a structure contains heavier elements. However, the benefits of invariom refinement, physically more meaningful ADPs, better accuracy in bond distances and the correction of asphericity shifts remain even when *R*-factor improvements are modest.

This work was supported by the Australian Synchrotron Research Program, which is funded by the Commonwealth of Australia under the Major National Research Facilities Program. BD thanks the ASRP for a postdoctoral fellowship and F. P. A. Fabbiani for reading and correcting the manuscript.

References

Allen, F. H. (2002). *Acta Cryst.* B**58**, 380–388.
Burnett, M. N. & Johnson, C. K. (1996). *ORTEP*III, Technical Report ORNL-6895. Oak Ridge National Laboratory, Tennessee, USA.
Brock, C. P., Dunitz, J. D. & Hirshfeld, F. L. (1991). *Acta Cryst.* B**47**, 789–797.
Chiba, A., Ueki, T., Ashida, T., Sasada, Y. & Kakudo, M. (1967). *Acta Cryst.* B**22**, 863–870.
Clark, R. C. & Reid, J. S. (1995). *Acta Cryst.* A**51**, 887–897.
Cruickshank, D. W. J. (1999). *Acta Cryst.* D**55**, 583–601.
Dittrich, B., Hübschle, C. B., Luger, P. & Spackman, M. A. (2006). *Acta Cryst.* D**62**, 1325–1335.
Dittrich, B., Hübschle, C. B., Messerschmidt, M., Kalinowski, R., Girnt, D. & Luger, P. (2005). *Acta Cryst.* A**61**, 314–320.
Dittrich, B., Koritsánszky, T. & Luger, P. (2004). *Angew. Chem. Int. Ed.* **43**, 2718–2721.

Dittrich, B., Munshi, P. & Spackman, M. A. (2006). *Acta Cryst.* C**62**, o633–o635.
Dittrich, B., Strümpel, M., Koritsánszky, T., Schäfer, M. & Spackman, M. A. (2006). *Acta Cryst.* A**62**, 217–223.
Flack, H. D. (1983). *Acta Cryst.* A**39**, 876–881.
Frisch, M. J. *et al.* (2002). *GAUSSIAN*98, Revision A.11.3. Gaussian Inc., Pittsburgh PA, USA.
Hansen, N. K. & Coppens, P. (1978). *Acta Cryst.* A**34**, 909–921.
Hirshfeld, F. L. (1976). *Acta Cryst.* A**32**, 239–244.
Hübschle, C. B., Dittrich, B. & Luger, P. (2007). *J. Appl. Cryst.* In the press.
Jelsch, C., Pichon-Pesme, V., Lecomte, C. & Aubry, A. (1998). *Acta Cryst.* D**54**, 1306–1318.
Kingsford-Adaboh, R., Dittrich, B., Hübschle, C. B., Gbewonyo, W. S. K., Okamoto, H., Kimura, M. & Ishida, H. (2006). *Acta Cryst.* B**62**, 843–849.
Koritsánszky, T., Richter, T., Macchi, P., Volkov, A., Gatti, C., Howard, S., Mallinson, P. R., Farrugia, L., Su, Z. W. & Hansen, N. K. (2003). *XD*. Freie Universität Berlin, Germany.
Koritsánszky, T., Volkov, A. & Coppens, P. (2002). *Acta Cryst.* A**58**, 464–472.
Oxford Diffraction Ltd (2006). *CrysAlis CCD* and *RED*, Version 1.171.31.5. Oxford Diffraction Ltd, Oxford.
Sheldrick, G. M. (1997). *SHELXL*97. University of Göttingen, Germany.
Spek, A. L. (2003). *J. Appl. Chem.* **36**, 7–13.
Stevens, E. D. & Coppens, P. (1976). *Acta Cryst.* A**32**, 915–917.
Volkov, A., Messerschmidt, M. & Coppens, P. (2007). *Acta Cryst.* D**63**, 160–170.
Westrip, S. P. (2007). *publCIF*. In preparation.
Zarychta, B., Pichon-Pesme, V., Guillot, B., Lecomte, C. & Jelsch, C. (2007). *Acta Cryst.* A**63**, 108–125.